



Geophysical Research Letters

RESEARCH LETTER

10.1029/2018GL079517

Key Points:

- Coastal western Greenland summers became cooler and more arid 9,000 to 8,000 years ago
- Wetter summers 8,000 years ago were synchronous with warming on western Greenland and throughout Northern Hemisphere
- Precipitation isotopes show wetter summers caused by increased local evaporation and increased poleward moisture transport

Supporting Information:

- Supporting Information S1

Correspondence to:

E. K. Thomas,
ekthomas@buffalo.edu

Citation:

Thomas, E. K., Castañeda, I. S., McKay, N. P., Briner, J. P., Salacup, J. M., Nguyen, K. Q., & Schweinsberg, A. D. (2018). A wetter Arctic coincident with hemispheric warming 8,000 years ago. *Geophysical Research Letters*, 45. <https://doi.org/10.1029/2018GL079517>

Received 6 JUL 2018

Accepted 24 SEP 2018

Accepted article online 1 OCT 2018

A Wetter Arctic Coincident With Hemispheric Warming 8,000 Years Ago

E. K. Thomas^{1,2} , I. S. Castañeda², N. P. McKay³ , J. P. Briner¹ , J. M. Salacup² , K. Q. Nguyen², and A. D. Schweinsberg¹

¹Department of Geology, University at Buffalo, Buffalo, NY, USA, ²Department of Geosciences, University of Massachusetts, Amherst, MA, USA, ³School of Earth Sciences and Environmental Sustainability, Northern Arizona University, Flagstaff, AZ, USA

Abstract Arctic precipitation is predicted to increase this century, with dramatic consequences for high-latitude systems. Observations remain spatiotemporally limited, hampering determination of the forcings causing wetter Arctic conditions, although two mechanisms have been proposed: enhanced local evaporation and greater poleward atmospheric moisture transport. Here a subcentennial-resolution multiproxy lake sediment record from western Greenland sheds light on these mechanisms. Cool summers throughout the Northern Hemisphere and in western Greenland 9 to 8 ka are associated with aridity in this region, via reductions in local evaporation and in meridional moisture gradients, which suppressed poleward moisture transport. Summers became more humid starting 8.1 ka, mainly due to increased evaporation from warmer Arctic seas but also to increased poleward moisture transport caused by hemispheric warming. This record provides independent support for predictions of both enhanced local evaporation and increased poleward moisture transport causing wetter Arctic summers in step with global ocean and atmosphere warming.

Plain Language Summary As the Arctic warms, it is getting wetter. This change can amplify warming worldwide by causing more plants to grow and decompose, releasing heat-trapping gases into the atmosphere. Sparse modern weather records in the Arctic make it difficult to pinpoint the forces causing increased rainfall, but scientists are debating two theories: (1) More water evaporates from warm, ice-free Arctic seas, and then falls locally as precipitation, or (2) as Earth warms, humidity rises more at lower latitudes, creating an imbalance that draws moist air up into the drier Arctic. Our research turns to history for insights. We show that in western Greenland, summers became cooler and drier about 9,000 years ago, coinciding with a drop in moisture imported from lower latitudes. Then, around 8,000 years ago, the region warmed rapidly and summers got wetter. A rise in both local evaporation and incoming moisture from lower latitudes may have fueled this change, according to our interpretation of geologic records. Our study suggests that both processes may contribute to a future, wetter Arctic. In addition, we advance scientific inquiry by using a recently developed technique, analysis of the hydrogen isotopes of ancient precipitation, to examine prehistoric humidity and precipitation trends that previously eluded investigation.

1. Introduction

Precipitation exerts strong impacts on, and feedback with, multiple aspects of the Arctic, including economic sectors, marine and terrestrial ecosystems, and the cryosphere (Larsen et al., 2014; Vaughan et al., 2013; Wrona et al., 2016). Recent sea ice loss and increases in Arctic river discharge have spurred interest in high-latitude precipitation (Kopec et al., 2016; National Snow and Ice Data Center, 2018; Zhang et al., 2013), which is predicted to increase by 2100 CE (Bintanja & Selten, 2014). There are two possible causes of increased high-latitude precipitation: enhanced dynamic poleward atmospheric moisture transport (hereafter, poleward moisture transport) or increased evaporation from warmer Arctic seas (Bintanja & Selten, 2014; Kopec et al., 2016; Zhang et al., 2013). Short observational records make it difficult to determine which of these causes dominates Arctic precipitation change (Dufour et al., 2016). Despite its potential importance, observed trends in poleward moisture transport are poorly represented in general circulation models and reanalysis data sets (Bintanja & Selten, 2014; Dufour et al., 2016; Frankenberg et al., 2009). Moreover, although seasonal precipitation changes may be caused by different mechanisms (Bintanja & Selten, 2014; Skific & Francis, 2013), observations rarely examine seasonal variability (Kopec et al., 2016; Screen & Simmonds,

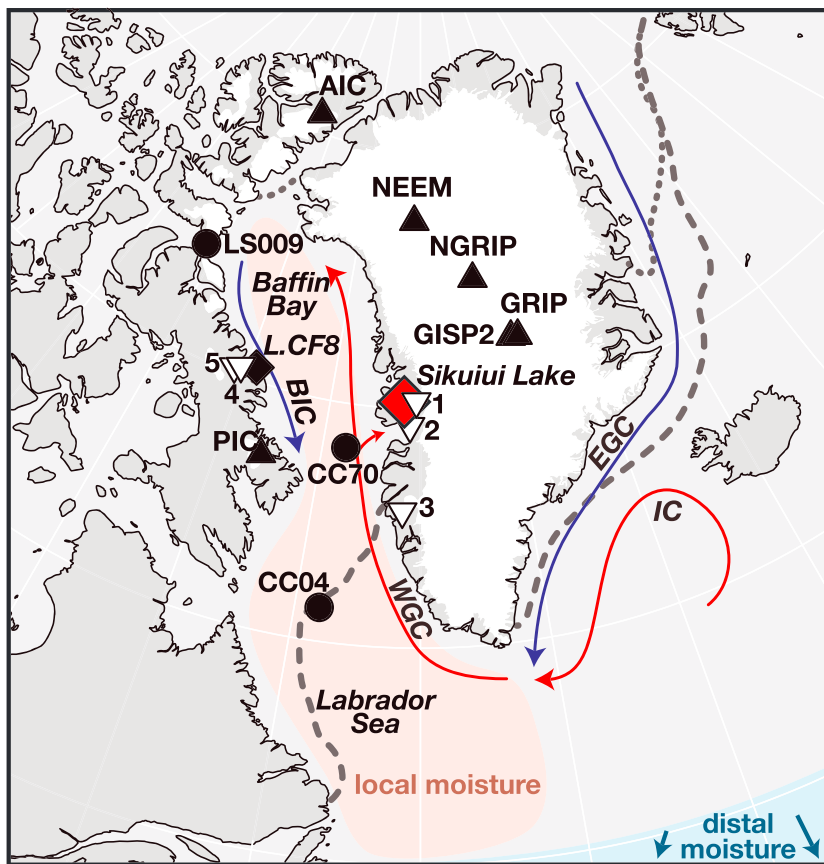


Figure 1. Map of study region. Sikuli Lake (red diamond), Lake CF8 (black diamond; Axford et al., 2009), early Holocene glacial deposits (white triangles; 1, Drygalski Moraines, Cronauer et al., 2016; 2 and 3 Fjord Stade Moraines, Lesnek & Briner, 2018; Young et al., 2011; 4 Ayr Lake, Young et al., 2012; and 5 Sam Ford Fiord, Briner et al., 2009), ice cores (black triangles), marine cores (black circles), ocean surface currents (warm currents red, cool currents blue), median winter (gray dashed lines), and summer (gray dotted lines) sea ice extent CE 1981–2010 (National Snow and Ice Data Center, 2018). Approximate regions of local (orange) and distal (blue; $<50^{\circ}\text{N}$; Sime et al., 2013) moisture sources to western Greenland. AIC, Agassiz Ice Cap; PIC, Penny Ice Cap; BIC, Baffin Island Current; WGC, West Greenland Current; EGC, East Greenland Current; IC, Irminger Current.

2012; Zhang et al., 2013). There is a critical need for longer data sets of seasonal Arctic climate to assess model predictions, particularly during periods of warm climate and abrupt change, which serve as partial analogs for the future.

We reconstruct summer temperature, precipitation hydrogen isotopic composition ($\delta^{2\text{H}}$), and aridity on western Greenland (Figure 1). Today, western Greenland precipitation is derived from local evaporation from the Labrador Sea and Baffin Bay and from poleward moisture transport via cyclones passing through the Labrador Sea and into Baffin Bay (Bintanja & Selten, 2014; Dufour et al., 2016; Sodemann et al., 2008). Our records span 9.5 to 7.2 ka (ka = thousand years before 1950 CE), a period of relative warmth in the Arctic (Kaufman et al., 2004) and western Greenland (Briner et al., 2016; McFarlin et al., 2018), which was punctuated by abrupt cold events at 9.2 and 8.2 ka (Alley & Ágústsdóttir, 2005; Kobashi et al., 2017). Ice cores provide high-resolution records of temperature, ice accumulation, and precipitation $\delta^{2\text{H}}$ and oxygen isotopes ($\delta^{18\text{O}}$) but are confined to high-elevation sites near the center of ice sheets and ice caps, and cover only a fraction of the terrestrial Arctic. Ice accumulation across the Greenland Ice Sheet reached a Holocene maximum around 8 ka, with lower values during the 8.2 ka event (Cuffey & Clow, 1997; Dahl-Jensen et al., 1993; Rasmussen et al., 2013). Ice core $\delta^{18\text{O}}$ and deuterium-excess show cooling and spatial variability in moisture sources across Greenland and the Canadian Arctic during the 9.2 and 8.2 ka events, suggesting a complex and widespread response across the high latitudes (Alley & Ágústsdóttir, 2005; Fisher et al., 1998; Lecavalier et al., 2017; Masson-Delmotte et al., 2005; Stuiver et al., 1995; Vinther et al., 2008).

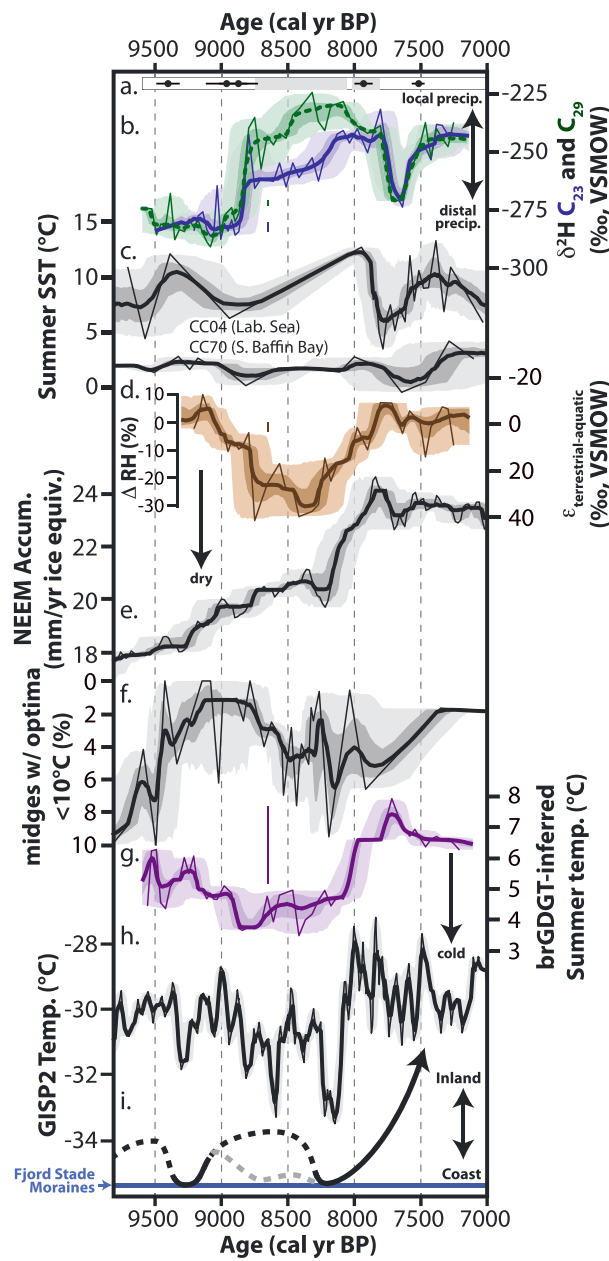


Figure 2. Select climate records from 9.7 to 7.0 ka in Baffin Bay region. (a) Sikuiui Lake stratigraphy (white: gyttja; gray: silty gyttja), radiocarbon ages (\pm 2 sigma uncertainty; Schweinsberg et al., 2017); (b) Sikuiui Lake leaf wax $\delta^2\text{H}$, C_{23} (aquatic): solid blue line, C_{29} (terrestrial): dashed green line; (c) Labrador Sea and Baffin Bay summer SST (Gibb et al., 2015); (d) Sikuiui Lake $\epsilon_{\text{terrestrial-aquatic}}$ inferred relative humidity (RH) anomalies relative to 7.8 to 7.3 ka mean; (e) NEEM accumulation (Rasmussen et al., 2013); (f) Lake CF8 cold stenothermic chironomids are more abundant during cold intervals, y-axis reversed (Axford et al., 2009); (g) Sikuiui Lake branched glycerol dialkyl glycerol tetraether-inferred summer temperature, the MBT'_{SME} calibration of Russell et al. (2018) was used; (h) GISP2 temperature (Kobashi et al., 2017); (i) time-distance diagram for Fjord Stade Moraines (Young et al., 2011). (b to h) The bold line represents median value of age model iterations; the fine line represents record on one age model; the light and dark shading represent 1 and 2 sigma age uncertainty, respectively (Comboul et al., 2014; McKay et al., 2018; McKay & Emile-Geay, 2016). The vertical colored bars in b, d, and e represent 1 sigma proxy uncertainty.

2. Methods and Approach

To quantify seasonal and spatiotemporal patterns of Arctic terrestrial climate variability, and to assess the mechanisms driving these patterns, we generated a subcentennial-resolution, multiproxy record at a low-elevation coastal site on western Greenland. We present organic geochemical records from a radiocarbon-dated sediment core from Sikuiui Lake on Nuussuaq (70.218°N , 51.123°W , 604 m above sea level; Figures 1, 2, and S1; Blaauw & Christen, 2011; Reimer et al., 2013; Schweinsberg et al., 2017; Thomas et al., 2018).

We use branched glycerol dialkyl glycerol tetraethers (brGDGTs; Buckles et al., 2014; De Jonge et al., 2014; Foster et al., 2016; Hopmans et al., 2016; Keisling et al., 2017; Loomis et al., 2012, 2014; Pearson et al., 2011; Schouten et al., 2002; Shanahan et al., 2013; Sun et al., 2011; Tierney et al., 2012; Weijers et al., 2007; de Wet et al., 2016) to reconstruct summer temperatures following a recently developed method that fully separates the 5- and 6-methyl brGDGT isomers (Hopmans et al., 2016) and applying the MBT'_{SME} index (De Jonge et al., 2014; supporting information). Presently, only two lake temperature calibrations exist for the MBT'_{SME} index that were developed using the same analytical method (Hopmans et al., 2016); one is based on alkaline Chinese lakes (Dang et al., 2018) and the other on African Lakes (Russell et al., 2018). As brGDGT distributions in Sikuiui Lake are distinct from those of the alkaline Chinese lakes (Dang et al., 2018) but similar to those from the African lakes (Russell et al., 2018), we chose to apply the Russell et al. (2018) temperature calibration (Supporting Information, Figure S2). Analysis of a Sikuiui Lake surface sediment sample yields a temperature of 0.7°C using this calibration, which is cooler than the early Holocene temperatures. We recognize that an African lakes calibration (Russell et al., 2018) may not be appropriate to apply to Arctic lakes but note that the calibration only influences the resulting absolute reconstructed temperature values. Therefore, we urge caution against interpreting the temperature values presented here, but nevertheless, trends in these data (i.e., the timing of warmings and coolings) remain robust (supporting information).

We use hydrogen isotope ratios of aquatic plant leaf waxes ($n\text{C}_{23}$, $\delta^2\text{H}_{\text{aq}}$; Aichner et al., 2017; Bennike, 2000; Daniels et al., 2017; Eglinton & Hamilton, 1967; ESRI, 2017; Ficken et al., 2000; Gao et al., 2011, 2014; Hou et al., 2007; Huang et al., 2004; Jonsson et al., 2009; Kahmen et al., 2013; Linderholm et al., 2018; Muschitiello et al., 2015; Nichols et al., 2009; Rach et al., 2014; Sachse et al., 2004, 2012; Thomas et al., 2014) to reconstruct Sikuiui Lake water $\delta^2\text{H}$ (Supporting Information, Figures S3–S5). Due to its small volume ($3.7 \times 10^{-4} \text{ km}^3$), Sikuiui Lake is rapidly flushed by spring snowmelt, and then continuously flushed by summer rainfall (Table S1). During relatively wet summers today, the lake has a 2-month residence time (Supporting Information, Table S1) and should be completely flushed by summer precipitation, meaning that $\delta^2\text{H}_{\text{aq}}$ reflects summer precipitation $\delta^2\text{H}$. During relatively dry summers today, the lake has an 8-month residence time (Table S1) and may only be partially flushed by summer precipitation, such that $\delta^2\text{H}_{\text{aq}}$ would reflect a mixture of summer and winter precipitation $\delta^2\text{H}$. The residence time of Sikuiui Lake is short enough that it likely does not experience evaporative enrichment (Jonsson et al., 2009). We therefore present two interpretations of Sikuiui Lake $\delta^2\text{H}_{\text{aq}}$: (1) $\delta^2\text{H}_{\text{aq}}$ reflects changes in summer precipitation $\delta^2\text{H}$ and (2) $\delta^2\text{H}_{\text{aq}}$ reflects

the proportion of summer precipitation amount relative to total annual precipitation amount.

Terrestrial plant leaf waxes in the Sikuiui Lake catchment are produced during the July to August growing season (Freimuth et al., 2017; Gao et al., 2012; ORNL DAAC, 2008). The hydrogen isotopes of terrestrial plant leaf waxes (nC_{29} , δ^2H_{ter}) reflect summer soil water δ^2H and leaf water evaporative 2H -enrichment, which increases as relative humidity (RH) decreases in midlatitudes and high latitudes (supporting information; Aichner et al., 2010; Bush et al., 2017; Rach et al., 2017; Shuman et al., 2006; Thomas et al., 2016). Summer soil water reflects summer precipitation δ^2H (Cooper et al., 1991).

All n -alkane chain lengths at Sikuiui Lake (C_{23} , C_{25} , C_{27} , and C_{29}) contain similar δ^2H values, and change at a similar time, except δ^2H_{C23} , which follows a similar pattern, but is 2H -depleted compared to the other chain lengths from approximately 9 to 8 ka (Figures 2 and S5). The unique pattern exhibited by nC_{23} compared to the longer chain lengths is consistent with a different source for this compound. The large, generally synchronous shifts that occur across chain lengths suggest that aquatic and terrestrial plants reflect similar seasonality. The similarities between δ^2H_{ter} , which reflects summer precipitation δ^2H , and δ^2H_{aq} support Interpretation 1 that δ^2H_{aq} reflects summer precipitation isotopes. Nevertheless, we discuss the implications of both interpretations.

If we assume that δ^2H_{aq} reflects summer precipitation δ^2H (Interpretation 1.), then the difference between δ^2H_{aq} and δ^2H_{ter} (ε_{ter-aq}) reflects the degree of evaporative 2H -enrichment of terrestrial plant leaf water. In this scenario, high ε_{ter-aq} values (i.e., δ^2H_{ter} is 2H -enriched relative to δ^2H_{aq}) indicate dry summers, and we can use ε_{ter-aq} and brGDGT-inferred temperature to infer past changes in summer RH (Rach et al., 2017). If we assume that δ^2H_{aq} reflects the proportion of summer precipitation amount (Interpretation 2.), then ε_{ter-aq} reflects the annual proportion of summer precipitation and terrestrial plant leaf water evaporation. In this scenario, high ε_{ter-aq} values reflect relatively dry summers (i.e., δ^2H_{ter} is 2H -enriched relative to δ^2H_{aq} because incomplete flushing of Sikuiui Lake water means the lake remains 2H -depleted). Thus, both possible interpretations of δ^2H_{aq} lead to the same inferred climate at this site.

3. Interpreting Greenland Precipitation Isotope Records: The Influence of Temperature, Moisture Source Isotopic Composition, and Transport History

Precipitation isotopes are affected by local condensation temperature, moisture transport history, and the isotopic composition of moisture sources (Dansgaard, 1964; Thomas et al., 2014). We assess the impact of each of these parameters on the Sikuiui Lake δ^2H and GISP2 $\delta^{18}O$ records. We remove the effect of local condensation temperature from Sikuiui Lake δ^2H_{aq} using brGDGT-inferred summer temperature and from GISP2 $\delta^{18}O$ using gas-fractionation-inferred annual air temperature (Kobashi et al., 2017; Stuiver et al., 1995; Figure 3; supporting information). Temperature changes from 9.7 to 7.0 ka at GISP2 and Sikuiui Lake had similar amplitudes (approximately 4 to 5 °C; Figure 2; Kobashi et al., 2017). We convert temperature to $\delta^{18}O$ using the average Greenland Holocene temperature— $\delta^{18}O$ relationship of 0.36‰/°C (Kobashi et al., 2017) and temperature to δ^2H using this same relationship multiplied by 8 (2.88‰/°C; Dansgaard, 1964). Local condensation temperature had a large impact on GISP2 $\delta^{18}O$ (Figures 3c and 3d; temperature y axis scaled to its effect on $\delta^{18}O$). ^{18}O -depleted events in the GISP2 temperature-corrected $\delta^{18}O$ record were synchronous with reconstructed freshwater inputs to the Labrador Sea and the North Atlantic Ocean (Jennings et al., 2015; Teller & Leverington, 2004; Törnqvist & Hijma, 2012; Figures 3c, 3e, and 3f). The synchronicity of the GISP2 $\delta^{18}O$ and freshwater records is consistent with model evidence that ^{18}O -depleted moisture source areas during freshwater pulses have an immediate, short-lived impact on Arctic precipitation $\delta^{18}O$ (LeGrande & Schmidt, 2008). Thus, local condensation temperature and moisture source $\delta^{18}O$ appear to strongly impact the high-elevation GISP2 $\delta^{18}O$ record, a pattern also observed in model sensitivity tests (Faber et al., 2017).

In contrast to the GISP2 $\delta^{18}O$ record, Sikuiui Lake δ^2H_{aq} was minimally impacted by local condensation temperature because the amplitude of the Sikuiui Lake δ^2H_{aq} record is much larger than the δ^2H changes caused by local condensation temperature (Figures 3a and 3b; temperature y axis scaled to its effect on δ^2H). Because both Sikuiui Lake δ^2H_{aq} and δ^2H_{ter} contain 25‰ shifts 8.8 and 7.7 ka, these large changes likely reflect changes in summer precipitation δ^2H . The changes in summer precipitation δ^2H do not coincide with regional freshwater pulses or with Laurentide Ice Sheet iceberg rafting in the Labrador Sea (Figures 3b, 3e, and 3f). Moreover, salinity in Baffin Bay was constant after 9.5 ka (Gibb et al., 2015), suggesting minimal changes in

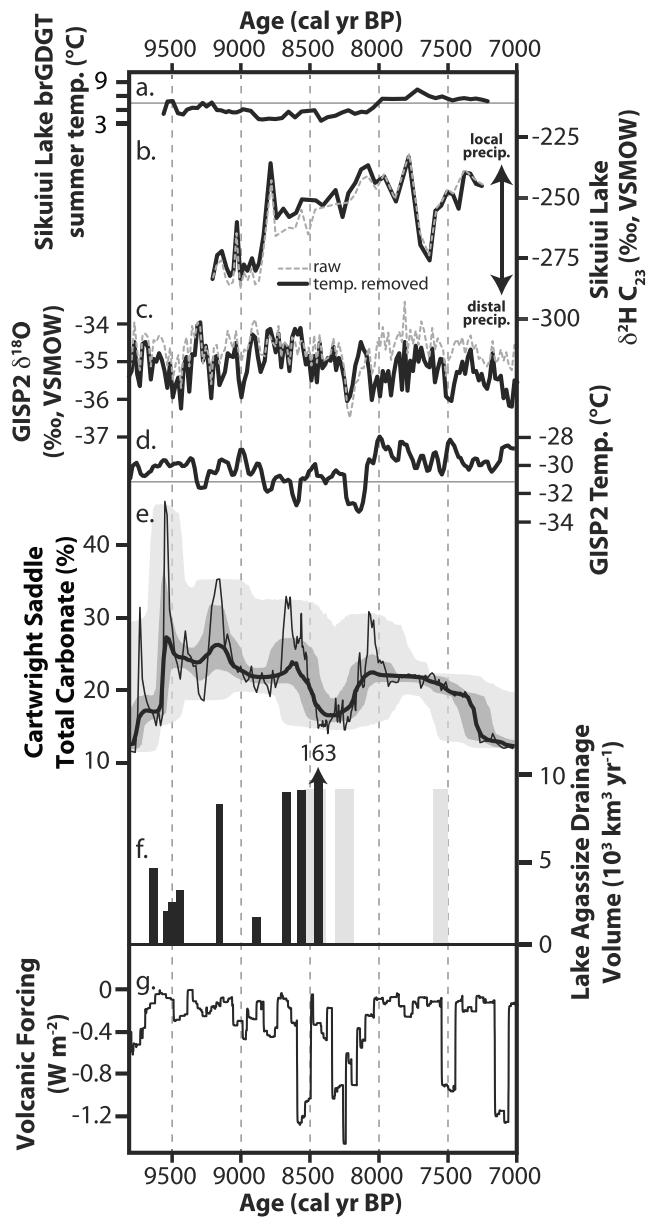


Figure 3. Greenland temperature and isotope records and forcing mechanisms. Temperature y axes scaled to magnitude of the isotope-temperature correction. Isotope y axes scaled to the same spacing ($\delta^2\text{H} = 8 \times \delta^{18}\text{O}$), but with GISP2 $\delta^{18}\text{O}_{\text{ice}}$ y axis amplified 2x. (a) Sikuli Lake branched glycerol dialkyl glycerol tetraether-inferred summer temperature; (b) Sikuli Lake $\delta^2\text{H}_{\text{aq}}$ with (solid line) and without (dashed line) the effects of local temperature removed; (c) GISP2 $\delta^{18}\text{O}_{\text{ice}}$ (Stuiver et al., 1995), lines as in b; (d) GISP2 temperature (Kobashi et al., 2017); (e) Labrador Sea carbonate abundance, indicating freshwater pulses from the Laurentide Ice Sheet (Jennings et al., 2015), uncertainty plotted like time series in Figure 2; (f) timing and volume of Lake Agassiz floods (black; Teller & Leverington, 2004) and timing of major sea level rises (gray; Törnqvist & Hijma, 2012); (g) volcanic forcing (Kobashi et al., 2017).

throughout the Northern Hemisphere 8.6 to 8.0 ka (Kobashi et al., 2017; Rohling & Pälike, 2005). Sustained summer cooling has been attributed to continuous freshwater input from waning ice sheets, solar, and/or volcanic forcing (Figure 3; Kobashi et al., 2017; Rohling & Pälike, 2005). The prolonged interval of cool, dry

freshwater input to, and $\delta^2\text{H}$ of, local moisture sources to western Greenland during our study interval. We therefore interpret the large changes in western Greenland summer precipitation $\delta^2\text{H}$ to indicate changes in moisture transport history, specifically relative changes in distal versus local moisture sources.

Moisture sources exert a major influence on precipitation isotope variability at high latitudes (Bowen, 2016; Bowen et al., 2005; IAEA/WMO, 2011; Kopec et al., 2014; NCEI NOAA, 2017; Noone, 2008; Sodemann et al., 2008; Werner et al., 2001). Continuous water vapor isotope measurements in Toolik, Alaska, show that moisture from the ice-free Arctic Ocean (local moisture) is more ^{18}O -enriched than moisture from the North Pacific Ocean (distal moisture; Klein et al., 2015). According to one model, distal moisture, derived from poleward moisture transport mainly from the Atlantic Ocean south of 50°N, becomes up to 40‰ ^{18}O -depleted compared to local moisture evaporated from the Labrador Sea and Baffin Bay (Sime et al., 2013). Using the global meteoric water $\delta^{18}\text{O}$ - $\delta^2\text{H}$ relationship (Dansgaard, 1964), this translates to a 320‰ difference in $\delta^2\text{H}$ between midlatitude and high-latitude moisture sources. Rayleigh distillation along the transport path to western Greenland causes the strong ^2H -depletion of distal moisture (Sime et al., 2013; Werner et al., 2001). While models only provide estimates of relative moisture source isotopic compositions, the large isotopic difference between source regions suggests that only minor changes in source area are needed to cause large changes in precipitation $\delta^2\text{H}$, which would be reflected in leaf wax $\delta^2\text{H}$, on western Greenland.

3.1. Western Greenland Climate 9.5 to 7.0 ka

We find that western Greenland experienced a prolonged period of cool, dry climate at 9 to 8 ka with warmer, wetter conditions before and after this period (Figures 2d and 2g). At 8.7 ka, when temperature was lowest and summers driest (i.e., high $\varepsilon_{\text{ter-aq}}$), a shift to ^2H -enriched values in Sikuli Lake $\delta^2\text{H}_{\text{aq}}$ and $\delta^2\text{H}_{\text{ter}}$ signaled a relative increase in the contribution of local moisture sources to western Greenland summer precipitation (Figure 2b). After the 8.2 ka event, western Greenland became warmer and wetter in step with warming throughout the North Atlantic region (Kobashi et al., 2017; Rohling & Pälike, 2005). A shift to ^2H -depleted leaf wax $\delta^2\text{H}$ at 7.6 to 7.5 ka suggests more distal moisture, which punctuated an otherwise stable mixture of distal and local moisture sources to western Greenland until the end of our record at 7.2 ka.

Our finding that western Greenland summers were cool from 9 to 8 ka is similar to other summer-sensitive proxies throughout Baffin Bay (Figure 2). Glaciers reached maximum extents on western Greenland and Baffin Island during this time (Figure 1; Briner et al., 2009; Cronauer et al., 2016; Young et al., 2011, 2012; Young & Briner, 2015). Cold stenothermic chironomid taxa at Lake CF8 on eastern Baffin Island were most abundant prior to 9.5 ka and 8.7 to 7.9 ka (Figure 2f, y axis reversed to be consistent with other temperature-sensitive proxies; Axford et al., 2009). The timing differences between lakes CF8 and Sikuli may be due to the influence of Atlantic water masses in eastern Baffin Bay versus Arctic water masses in western Baffin Bay (Figure 1). Cool and arid summers also occurred

summers on western Greenland contrasted with winter proxy records, which changed abruptly at 8.2 ka, driven by glacial lake outbursts or iceberg rafting events that caused Atlantic Meridional Overturning Circulation (AMOC) to weaken (Kobashi et al., 2017; Rohling & Pälike, 2005; Stuiver et al., 1995; Törnqvist & Hijma, 2012).

4. Hemispheric Summer Cooling Caused Decreased Poleward Moisture Transport

Our Sikuiui Lake reconstructions provide an opportunity to assess the mechanisms causing changes in Holocene RH and moisture sources on western Greenland. Prior to 6.8 ka, the West Greenland Current (Figure 1) was both weak and cool (Perner et al., 2013), and low Baffin Bay sea surface temperature (SST) until 7.5 ka suppressed evaporation (Figure 2C; Gibb et al., 2015). Thus, the apparent increased contribution of local moisture sources at 8.7 ka likely reflects decreased distal moisture transport to western Greenland. This decrease, in addition to minimal local moisture contributions, would cause drier conditions on western Greenland, consistent with low ϵ_{ter-aq} and low inferred RH at Sikuiui Lake (Figure 2d). A concurrent shift to ^{18}O -enriched values is not recorded in the GISP2 ice core (Figure 3d; Stuiver et al., 1995), perhaps because orographically induced ^{18}O -depletion during transport to high-elevation sites dominates the signal there (Faber et al., 2017). Deuterium-excess records at GRIP and NGRIP demonstrate complex spatiotemporal variability in moisture sources on centennial time scales, possibly indicating the dominance of local moisture sources to NGRIP and distal moisture sources to GRIP during the 8.5 to 8.0 ka cool period (Frankenberg et al., 2009; Masson-Delmotte et al., 2005).

An important driver of Early Holocene climate change, and a potential cause of moisture source shifts, is freshwater suppression of the AMOC in the North Atlantic (Alley & Ágústsdóttir, 2005; Masson-Delmotte et al., 2005). A weaker AMOC decreases ocean heat transport to high latitudes, which is partially compensated by increased atmospheric heat and moisture transport (LeGrande & Schmidt, 2008). Yet at Sikuiui Lake, we observe a decrease in distal moisture source contributions to summer precipitation, synchronous with cold, dry conditions (Figures 2b, 2d, and 2g). A weaker AMOC and consequent strengthened poleward moisture transport therefore was probably not the main cause of reconstructed arid summers on western Greenland 9 to 8 ka.

In contrast, cooling at both high and low latitudes decreases meridional atmospheric moisture gradients and, consequently, decreases poleward moisture transport (Sime et al., 2013; Skific & Francis, 2013). The relative decrease in distal moisture source contribution to Sikuiui Lake 8.7 ka is synchronous with cold conditions there and with the start of a prolonged cold period at GISP2 (Figures 2b, 2g, and 2h; Kobashi et al., 2017). A decrease in poleward moisture transport also requires cooling in low-latitude moisture source regions. There is evidence for low SSTs in the midlatitude and low-latitude North Atlantic region from 9 to 8 ka (Lea et al., 2003; Rohling & Pälike, 2005). This hemispheric-wide cooling likely decreased poleward moisture transport 8.7 ka and enhanced summer aridity on western Greenland.

5. Local and Distal Moisture Source Contributions to Western Greenland Increased as the Northern Hemisphere Warmed

Warming at Sikuiui Lake, Lake CF8, GISP2, and at low latitude and midlatitudes after 8.2 ka (Axford et al., 2009; Kobashi et al., 2017; Lea et al., 2003) likely enhanced distal moisture transport to western Greenland (Figure 2b). Yet the relative contribution of local moisture sources to western Greenland remained high after 8.2 ka. Baffin Bay summer SST remained low until 7.5 ka (Figure 2c; Gibb et al., 2015; Moros et al., 2016; Ouellet-Bernier et al., 2014), likely excluding Baffin Bay as a dominant local moisture source. The Labrador Sea, on the other hand, was relatively warm during this period (Gibb et al., 2015) and may have provided a local moisture source to western Greenland. Together, increased distal and local moisture transport would have made western Greenland more humid, consistent with higher ϵ_{ter-aq} values and increased RH (Figure 2d). A brief increase in distal moisture source relative contributions 7.7 ka coincided with lower summer SST in the Labrador Sea and Baffin Bay (Figures 2b and 2c; Gibb et al., 2015), which may have caused a decrease in local moisture evaporation. Continued warm conditions on Greenland (Figures 2g and 2h) and at low latitudes would have maintained poleward moisture transport during this period.

Like Sikuiui Lake, precipitation at the NEEM ice core site (Figure 1) occurs mainly during summer, with moisture from Baffin Bay and low-latitude sources (Rasmussen et al., 2013; Steen-Larsen et al., 2011).

Accumulation at NEEM increased gradually prior to 9.0 ka (Figure 2e), likely due to warming and sea ice retreat in northern Baffin Bay (Ledu et al., 2010). After 8.5 ka, NEEM accumulation had strong similarities with RH at Sikuiui Lake: both were low and generally stable 8.5 to 8.2 ka, increased 8.2 to 7.8 ka, and stabilized thereafter (Figures 2d and 2e). The similarity of the Sikuiui Lake RH and NEEM accumulation records provides further support for the interpretation that western Greenland summers were dry during prolonged cold conditions 9.0 to 8.0 ka, and subsequently became wetter as the region warmed and both distal moisture transport and local evaporation increased.

6. Conclusions

While the multiproxy approach we apply here cannot decipher the magnitude of poleward moisture transport or local moisture sources, application of this approach at sites throughout the Arctic may provide detailed descriptions of summer temperature, precipitation $\delta^2\text{H}$, aridity, and relative contributions of local and distal moisture sources during previous periods of abrupt climate change. Although attention has focused on the role of retreating sea ice cover and increasing local evaporation causing wetter Arctic winters (Bintanja & Selten, 2014; Faber et al., 2017; Kopec et al., 2016; Thomas et al., 2016), we suggest that western Greenland summers also underwent large changes in precipitation sources and aridity during the Holocene. This finding is consistent with fluctuations in poleward moisture transport caused by hemispheric temperature and moisture gradients and is inconsistent with moisture transport changes resulting from regional meltwater forcing. Additionally, this reconstruction provides independent evidence that both mechanisms proposed as drivers of future summer precipitation in the Arctic (Bintanja & Selten, 2014; Dufour et al., 2016; Kopec et al., 2016; Skific & Francis, 2013; Zhang et al., 2013), local evaporation and poleward moisture transport, operated in the past.

Today, poleward moisture transport mainly occurs during summer via cyclones concentrated at moisture gateways to the Arctic, including the Labrador Sea and the North Atlantic and North Pacific oceans (Dufour et al., 2016). We have demonstrated that western Greenland, just downwind of the Labrador Sea gateway, experienced increases in poleward moisture transport during previous periods of rapid warming. This and other gateway regions therefore may be particularly sensitive to future changes in poleward moisture transport, via increased cyclonic activity (Dufour et al., 2016). Ongoing warming and increased precipitation will drive complex responses in Arctic ecosystems, including increases in terrestrial and aquatic primary productivity and respiration (Larsen et al., 2014; Wrona et al., 2016). This, in turn, may drive increases in carbon remineralization, thus amplifying warming and wetting trends (Wrona et al., 2016).

Acknowledgments

This research was supported by NSF EAR Postdoctoral Research Fellowship 1349595 to E. K. T. and NSF grant ARC-1204005 to J. P. B. All samples are archived at the University at Buffalo Department of Geology, and new data from Sikuiui Lake presented in this paper are publicly available at the NOAA/NCDC Paleoclimate website: <https://www.ncdc.noaa.gov/paleo/study/24570>.

References

- Aichner, B., Herzschuh, U., Wilkes, H., Vieth, A., & Böhner, J. (2010). δD values of n-alkanes in Tibetan lake sediments and aquatic macrophytes – A surface sediment study and application to a 16 ka record from Lake Koucha. *Organic Geochemistry*, 41(8), 779–790. <https://doi.org/10.1016/j.orggeochem.2010.05.010>
- Aichner, B., Hilt, S., Périalon, C., Gillefalk, M., & Sachse, D. (2017). Biosynthetic hydrogen isotopic fractionation factors during lipid synthesis in submerged aquatic macrophytes: Effect of groundwater discharge and salinity. *Organic Geochemistry*, 113(Supplement C), 10–16. <https://doi.org/10.1016/j.orggeochem.2017.07.021>
- Alley, R. B., & Ágústsdóttir, A. M. (2005). The 8k event: Cause and consequences of a major Holocene abrupt climate change. *Quaternary Science Reviews*, 24(10–11), 1123–1149. <https://doi.org/10.1016/j.quascirev.2004.12.004>
- Axford, Y., Briner, J. P., Cooke, C. A., Francis, D. R., Michelutti, N., Miller, G. H., et al. (2009). Recent changes in a remote Arctic lake are unique within the past 200,000 years. *Proceedings of the National Academy of Sciences*, 106(44), 18,443–18,446. <https://doi.org/10.1073/pnas.0907094106>
- Bennike, O. (2000). Palaeoecological studies of Holocene lake sediments from west Greenland. *Palaeogeography, Palaeoclimatology, Palaeoecology*, 155(3–4), 285–304. [https://doi.org/10.1016/S0031-0182\(99\)00121-2](https://doi.org/10.1016/S0031-0182(99)00121-2)
- Bintanja, R., & Selten, F. M. (2014). Future increases in Arctic precipitation linked to local evaporation and sea-ice retreat. *Nature*, 509(7501), 479–482. <https://doi.org/10.1038/nature13259>
- Blaauw, M., & Christen, J. A. (2011). Flexible paleoclimate age-depth models using an autoregressive gamma process. *Bayesian Analysis*, 6(3), 457–474. <https://doi.org/10.1214/11-BA618>
- Bowen, G. J. (2016). OIPC: The online isotopes in precipitation calculator, version 2.2. Retrieved from www.waterisotopes.org
- Bowen, G. J., Wassenaar, L. I., & Hobson, K. A. (2005). Global application of stable hydrogen and oxygen isotopes to wildlife forensics. *Oecologia*, 143(3), 337–348.
- Briner, J. P., Bini, A. C., & Anderson, R. S. (2009). Rapid early Holocene retreat of a Laurentide outlet glacier through an Arctic fjord. *Nature Geoscience*, 2(7), 496–499. <https://doi.org/10.1038/nge0556>
- Briner, J. P., McKay, N. P., Axford, Y., Bennike, O., Bradley, R. S., de Vernal, A., et al. (2016). Holocene climate change in Arctic Canada and Greenland. *Quaternary Science Reviews*. <https://doi.org/10.1016/j.quascirev.2016.02.010>

- Buckles, L. K., Weijers, J. W. H., Verschuren, D., & Sinnenhe Damsté, J. S. (2014). Sources of core and intact branched tetraether membrane lipids in the lacustrine environment: Anatomy of Lake Challa and its catchment, equatorial East Africa. *Geochimica et Cosmochimica Acta*, 140, 106–126. <https://doi.org/10.1016/j.gca.2014.04.042>
- Bush, R. T., Berke, M. A., & Jacobson, A. D. (2017). Plant water δD and $\delta^{18}O$ of tundra species from West Greenland. *Arctic, Antarctic, and Alpine Research*, 49(3), 341–358. <https://doi.org/10.1657/AAAR0016-025>
- Comboul, M., Emile-Geay, J., Evans, M. N., Mirnateghi, N., Cobb, K. M., & Thompson, D. M. (2014). A probabilistic model of chronological errors in layer-counted climate proxies: Applications to annually banded coral archives. *Climate of the Past*, 10(2), 825–841. <https://doi.org/10.5194/cp-10-825-2014>
- Cooper, L. W., Olsen, C. R., Solomon, D. K., Larsen, I. L., Cook, R. B., & Grebmeier, J. M. (1991). Stable isotopes of oxygen and natural and fallout radionuclides used for tracing runoff during snowmelt in an Arctic Watershed. *Water Resources Research*, 27(9), 2171–2179. <https://doi.org/10.1029/91WR01243>
- Cronauer, S. L., Briner, J. P., Kelley, S. E., Zimmerman, S. R. H., & Morlighem, M. (2016). ^{10}Be dating reveals early-middle Holocene age of the Drygalski Moraines in central West Greenland. *Quaternary Science Reviews*, 147, 59–68. <https://doi.org/10.1016/j.quascirev.2015.08.034>
- Cuffey, K. M., & Clow, G. D. (1997). Temperature, accumulation, and ice sheet elevation in central Greenland through the last deglacial transition. *Journal of Geophysical Research*, 102(C12), 26,383–26,396. <https://doi.org/10.1029/96JC03981>
- Dahl-Jensen, D., Johnsen, S. J., Hammer, C. U., Clausen, H. B., & Jouzel, J. (1993). Past Accumulation rates derived from observed annual layers in the GRIP ice core from Summit, Central Greenland. In W. R. Peltier (Ed.), *Ice in the Climate System*, (pp. 517–532). Berlin, Heidelberg: Springer Berlin Heidelberg. <https://doi.org/10.1007/978-3-642-85016-5>
- Dang, X., Ding, W., Yang, H., Pancost, R. D., Naafs, B. D. A., Xue, J., et al. (2018). Different temperature dependence of the bacterial brGDGT isomers in 35 Chinese lake sediments compared to that in soils. *Organic Geochemistry*, 119, 72–79. <https://doi.org/10.1016/j.orggeochem.2018.02.008>
- Daniels, W. C., Russell, J. M., Giblin, A. E., Welker, J. M., Klein, E. S., & Huang, Y. (2017). Hydrogen isotope fractionation in leaf waxes in the Alaskan Arctic tundra. *Geochimica et Cosmochimica Acta*, 213, 216–236. <https://doi.org/10.1016/j.gca.2017.06.028>
- Dansgaard, W. (1964). Stable isotopes in precipitation. *Tellus*, 16(4), 436–468. <https://doi.org/10.1111/j.2153-3490.1964.tb00181.x>
- De Jonge, C., Hopmans, E. C., Zell, C. I., Kim, J.-H., Schouten, S., & Sinnenhe Damsté, J. S. (2014). Occurrence and abundance of 6-methyl branched glycerol dialkyl glycerol tetraethers in soils: Implications for palaeoclimate reconstruction. *Geochimica et Cosmochimica Acta*, 141, 97–112. <https://doi.org/10.1016/j.gca.2014.06.013>
- de Wet, G. A., Castañeda, I. S., DeConto, R. M., & Brigham-Grette, J. (2016). A high-resolution mid-Pleistocene temperature record from Arctic Lake El'gygytgyn: a 50 kyr super interglacial from MIS 33 to MIS 31? *Earth and Planetary Science Letters*, 436, 56–63. <https://doi.org/10.1016/j.epsl.2015.12.021>
- Dufour, A., Zolina, O., & Gulev, S. K. (2016). Atmospheric moisture transport to the Arctic: Assessment of reanalyses and analysis of transport components. *Journal of Climate*, 29(14), 5061–5081. <https://doi.org/10.1175/JCLI-D-15-0559.1>
- Eglinton, G., & Hamilton, R. J. (1967). Leaf epicuticular waxes. *Science*, 156(3780), 1322–1335.
- ESRI (2017). *ArcGIS desktop (Version Release 10.5.1)*. Redlands, CA: Environmental Systems Research Institute.
- Faber, A.-K., Møllesøe Vinther, B., Sjolte, J., & Anker Pedersen, R. (2017). How does sea ice influence $\delta^{18}O$ of Arctic precipitation? *Atmospheric Chemistry and Physics*, 17(9), 5865–5876. <https://doi.org/10.5194/acp-17-5865-2017>
- Ficken, K. J., Li, B., Swain, D. L., & Eglinton, G. (2000). An n-alkane proxy for the sedimentary input of submerged/floating freshwater aquatic macrophytes. *Organic Geochemistry*, 31(7–8), 745–749. [https://doi.org/10.1016/S0146-6380\(00\)00081-4](https://doi.org/10.1016/S0146-6380(00)00081-4)
- Fisher, D. A., Koerner, R. M., Bourgeois, J. C., Zielinski, G., Wake, C., Hammer, C. U., et al. (1998). Penny Ice Cap Cores, Baffin Island, Canada, and the Wisconsinan Foxe Dome Connection: Two States of Hudson Bay Ice Cover. *Science*, 279(5351), 692–695. <https://doi.org/10.1126/science.279.5351.692>
- Foster, L. C., Pearson, E. J., Juggins, S., Hodgson, D. A., Saunders, K. M., Verleyen, E., et al. (2016). Development of a regional glycerol dialkyl glycerol tetraether (GDGT)-temperature calibration for Antarctic and sub-Antarctic lakes. *Earth and Planetary Science Letters*, 433, 370–379. <https://doi.org/10.1016/j.epsl.2015.11.018>
- Frankenberg, C., Yoshimura, K., Warneke, T., Aben, I., Butz, A., Deutscher, N., et al. (2009). Dynamic processes governing lower-tropospheric HDO/H₂O ratios as observed from space and ground. *Science*, 325(5946), 1374–1377. <https://doi.org/10.1126/science.1173791>
- Freimuth, E. J., Diefendorf, A. F., & Lowell, T. V. (2017). Hydrogen isotopes of n-alkanes and n-alkanoic acids as tracers of precipitation in a temperate forest and implications for paleorecords. *Geochimica et Cosmochimica Acta*, 206, 166–183. <https://doi.org/10.1016/j.gca.2017.02.027>
- Gao, L., Burnier, A., & Huang, Y. (2012). Quantifying instantaneous regeneration rates of plant leaf waxes using stable hydrogen isotope labeling. *Rapid Communications in Mass Spectrometry*, 26(2), 115–122. <https://doi.org/10.1002/rcm.5313>
- Gao, L., Edwards, E. J., Zeng, Y., & Huang, Y. (2014). Major evolutionary trends in hydrogen isotope fractionation of vascular plant leaf waxes. *PLoS ONE*, 9(11), e112610. <https://doi.org/10.1371/journal.pone.0112610>
- Gao, L., Hou, J., Toney, J., MacDonald, D., & Huang, Y. (2011). Mathematical modeling of the aquatic macrophyte inputs of mid-chain n-alkyl lipids to lake sediments: Implications for interpreting compound specific hydrogen isotopic records. *Geochimica et Cosmochimica Acta*, 75, 3781–3791.
- Gibb, O. T., Steinhauer, S., Fréchette, B., de Vernal, A., & Hillaire-Marcel, C. (2015). Diachronous evolution of sea surface conditions in the Labrador Sea and Baffin Bay since the last deglaciation. *The Holocene*, 25(12), 1882–1897. <https://doi.org/10.1177/0959683615591352>
- Hopmans, E. C., Schouten, S., & Sinnenhe Damsté, J. S. (2016). The effect of improved chromatography on GDGT-based palaeoproxies. *Organic Geochemistry*, 93, 1–6. <https://doi.org/10.1016/j.orggeochem.2015.12.006>
- Hou, J., D'Andrea, W. J., MacDonald, D., & Huang, Y. (2007). Hydrogen isotopic variability in leaf waxes among terrestrial and aquatic plants around Blood Pond, Massachusetts (USA). *Organic Geochemistry*, 38(6), 977–984. <https://doi.org/10.1016/j.orggeochem.2006.12.009>
- Huang, Y., Shuman, B., Wang, Y., & Webb, T. (2004). Hydrogen isotope ratios of individual lipids in lake sediments as novel tracers of climatic and environmental change: a surface sediment test. *Journal of Paleolimnology*, 31(3), 363–375.
- IAEA/WMO (2011). Global Network of Isotopes in Precipitation. The GNIP database. Retrieved from <http://www.iaea.org/water>
- Jennings, A., Andrews, J., Pearce, C., Wilson, L., & Ólfasdóttir, S. (2015). Detrital carbonate peaks on the Labrador shelf, a 13–7 ka template for freshwater forcing from the Hudson Strait outlet of the Laurentide Ice Sheet into the subpolar gyre. *Quaternary Science Reviews*, 107, 62–80. <https://doi.org/10.1016/j.quascirev.2014.10.022>
- Jonsson, C. E., Leng, M. J., Rosqvist, G. C., Seibert, J., & Arrowmith, C. (2009). Stable oxygen and hydrogen isotopes in sub-Arctic lake waters from northern Sweden. *Journal of Hydrology*, 376(1–2), 143–151. <https://doi.org/10.1016/j.jhydrol.2009.07.021>
- Kahmen, A., Schefuß, E., & Sachse, D. (2013). Leaf water deuterium enrichment shapes leaf wax n-alkane δD values of angiosperm plants I: Experimental evidence and mechanistic insights. *Geochimica et Cosmochimica Acta*, 111, 39–49. <https://doi.org/10.1016/j.gca.2012.09.003>

- Kaufman, D. S., Ager, T. A., Anderson, N. J., Anderson, P. M., Andrews, J. T., Bartlein, P. J., et al. (2004). Holocene thermal maximum in the western Arctic (0–180°W). *Quaternary Science Reviews*, 23(5–6), 529–560. <https://doi.org/10.1016/j.quascirev.2003.09.007>
- Keisling, B. A., Castañeda, I. S., & Brigham-Grette, J. (2017). Hydrological and temperature change in Arctic Siberia during the intensification of Northern Hemisphere Glaciation. *Earth and Planetary Science Letters*, 457, 136–148. <https://doi.org/10.1016/j.epsl.2016.09.058>
- Klein, E. S., Cherry, J. E., Young, J., Noone, D., Leffler, A. J., & Welker, J. M. (2015). Arctic cyclone water vapor isotopes support past sea ice retreat recorded in Greenland ice. *Scientific Reports*, 5, 10295. <https://doi.org/10.1038/srep10295>
- Kobashi, T., Menviel, L., Jeltsch-Thömmes, A., Vinther, B. M., Box, J. E., Muscheler, R., et al. (2017). Volcanic influence on centennial to millennial Holocene Greenland temperature change. *Scientific Reports*, 7(1), 1441. <https://doi.org/10.1038/s41598-017-01451-7>
- Kopecky, B. G., Feng, X., Michel, F. A., & Posmentier, E. S. (2016). Influence of sea ice on Arctic precipitation. *Proceedings of the National Academy of Sciences*, 113(1), 46–51. <https://doi.org/10.1073/pnas.1504633113>
- Kopecky, B. G., Lauder, A. M., Posmentier, E. S., & Feng, X. (2014). The diel cycle of water vapor in west Greenland. *Journal of Geophysical Research: Atmospheres*, 119, 9386–9399. <https://doi.org/10.1002/2014JD021859>
- Larsen, J. N., Anisimov, O. A., Constable, A., Hollowed, A. B., Maynard, N., Prestrud, P., et al. (2014). Polar Regions. In V. R. Barros, C. B. Field, D. J. Dokken, M. D. Mastrandrea, K. J. Mach, T. E. Bilir, et al. (Eds.), *Climate change 2014: Impacts, adaptation, and vulnerability. Part B: Regional aspects. Contribution of Working Group II to the Fifth Assessment Report of the Intergovernmental Panel on Climate Change*, (pp. 1567–1612). Cambridge, UK and New York, NY, USA: Cambridge Univ. Press. Retrieved from https://www.ipcc.ch/pdf/assessment-report/ar5/wg2/WGIIAR5-Chap28_FINAL.pdf
- Lea, D. W., Pak, D. K., Peterson, L. C., & Hughen, K. A. (2003). Synchronicity of tropical and high-latitude Atlantic temperatures over the Last Glacial Termination. *Science*, 301(5638), 1361–1364. <https://doi.org/10.1126/science.1088470>
- LeCavalier, B. S., Fisher, D. A., Milne, G. A., Vinther, B. M., Tarasov, L., Huybrechts, P., et al. (2017). High Arctic Holocene temperature record from the Agassiz ice cap and Greenland ice sheet evolution. *Proceedings of the National Academy of Sciences*, 201616287. <https://doi.org/10.1073/pnas.1616287114>
- Ledu, D., Rochon, A., de Vernal, A., Barletta, F., & St-Onge, G. (2010). Holocene sea ice history and climate variability along the main axis of the Northwest Passage, Canadian Arctic. *Paleoceanography*, 25, PA2213. <https://doi.org/10.1029/2009PA001817>
- LeGrande, A. N., & Schmidt, G. A. (2008). Ensemble, water isotope-enabled, coupled general circulation modeling insights into the 8.2 ka event. *Paleoceanography*, 23, PA3207. <https://doi.org/10.1029/2008PA001610>
- Lesnek, A. J., & Briner, J. P. (2018). Response of a land-terminating sector of the western Greenland Ice Sheet to early Holocene climate change: Evidence from 10 Be dating in the Søndre Isortoq region. *Quaternary Science Reviews*, 180, 145–156. <https://doi.org/10.1016/j.quascirev.2017.11.028>
- Linderholm, H. W., Nicolle, M., Francus, P., Gajewski, K., Helama, S., Korhola, A., et al. (2018). Arctic hydroclimate variability during the last 2000 years: current understanding and research challenges. *Climate of the Past*, 14(4), 473–514. <https://doi.org/10.5194/cp-14-473-2018>
- Loomis, S. E., Russell, J. M., Heureux, A. M., D'Andrea, W. J., & Sinnenhe Damsté, J. S. (2014). Seasonal variability of branched glycerol dialkyl glycerol tetraethers (brGDGTs) in a temperate lake system. *Geochimica et Cosmochimica Acta*, 144, 173–187. <https://doi.org/10.1016/j.gca.2014.08.027>
- Loomis, S. E., Russell, J. M., Ladd, B., Street-Perrott, F. A., & Sinnenhe Damsté, J. S. (2012). Calibration and application of the branched GDGT temperature proxy on East African lake sediments. *Earth and Planetary Science Letters*, 357–358, 277–288. <https://doi.org/10.1016/j.epsl.2012.09.031>
- Masson-Delmotte, V., Landais, A., Steivensard, M., Cattani, O., Falourd, S., Jouzel, J., et al. (2005). Holocene climatic changes in Greenland: Different deuterium excess signals at Greenland Ice Core Project (GRIP) and NorthGRIP. *Journal of Geophysical Research*, 110, D14102. <https://doi.org/10.1029/2004JD005575>
- McFarlin, J. M., Axford, Y., Osburn, M. R., Kelly, M. A., Osterberg, E. C., & Farnsworth, L. B. (2018). Pronounced summer warming in northwest Greenland during the Holocene and Last Interglacial. *Proceedings of the National Academy of Sciences*, 201720420. <https://doi.org/10.1073/pnas.1720420115>
- McKay, N. P., & Emile-Geay, J. (2016). Technical note: The Linked Paleo Data framework – a common tongue for paleoclimatology. *Climate of the Past*, 12(4), 1093–1100. <https://doi.org/10.5194/cp-12-1093-2016>
- McKay, N. P., Emile-Geay, J., Heiser, C., & Khider, D. (2018). GeoChronR development repository. doi:<https://doi.org/10.5281/zenodo.60812>.
- Moros, M., Lloyd, J. M., Perner, K., Krawczyk, D., Blanz, T., de Vernal, A., et al. (2016). Surface and sub-surface multi-proxy reconstruction of middle to late Holocene palaeoceanographic changes in Disko Bugt, West Greenland. *Quaternary Science Reviews*, 132, 146–160. <https://doi.org/10.1016/j.quascirev.2015.11.017>
- Muschitiello, F., Pausata, F. S. R., Watson, J. E., Smittenberg, R. H., Salih, A. A. M., Brooks, S. J., et al. (2015). Fennoscandian freshwater control on Greenland hydroclimate shifts at the onset of the Younger Dryas. *Nature Communications*, 6, 8939. <https://doi.org/10.1038/ncomms9939>
- National Snow and Ice Data Center (2018). SOTC: Sea ice. Retrieved from http://nsidc.org/cryosphere/sotc/sea_ice.html
- NCEI NOAA (2017). Global historical climatology network. National Centers for Environmental Information, National Oceanic and Atmospheric Administration. Retrieved from <http://www.ncdc.noaa.gov/oa/climate/ghcn-daily/>
- Nichols, J. E., Walcott, M., Bradley, R., Pilcher, J., & Huang, Y. (2009). Quantitative assessment of precipitation seasonality and summer surface wetness using ombrotrophic sediments from an Arctic Norwegian peatland. *Quaternary Research*, 72(3), 443–451. <https://doi.org/10.1016/j.yqres.2009.07.007>
- Noone, D. (2008). The influence of midlatitude and tropical overturning circulation on the isotopic composition of atmospheric water vapor and Antarctic precipitation. *Journal of Geophysical Research*, 113, D04102. <https://doi.org/10.1029/2007JD008892>
- ORNL DAAC (2008). MODIS Collection 5 land products global subsetting and visualization tool. Oak Ridge, Tennessee, USA: Oak Ridge National Laboratory Distributed Active Archive Center. <https://doi.org/10.3334/ORNLDAA/1241>
- Ouellet-Bernier, M.-M., de Vernal, A., Hillaire-Marcel, C., & Moros, M. (2014). Paleoceanoceanographic changes in the Disko Bugt area, West Greenland, during the Holocene. *The Holocene*, 24(11), 1573–1583. <https://doi.org/10.1177/0959683614544060>
- Pearson, E. J., Juggins, S., Talbot, H. M., Weckström, J., Rosén, P., Ryves, D. B., et al. (2011). A lacustrine GDGT-temperature calibration from the Scandinavian Arctic to Antarctic: Renewed potential for the application of GDGT-paleothermometry in lakes. *Geochimica et Cosmochimica Acta*, 75(20), 6225–6238. <https://doi.org/10.1016/j.gca.2011.07.042>
- Perner, K., Moros, M., Jennings, A., Lloyd, J. M., & Knudsen, K. L. (2013). Holocene palaeoceanographic evolution off West Greenland. *The Holocene*, 23(3), 374–387. <https://doi.org/10.1177/0959683612460785>
- Rach, O., Brauer, A., Wilkes, H., & Sachse, D. (2014). Delayed hydrological response to Greenland cooling at the onset of the Younger Dryas in western Europe. *Nature Geoscience*, 7(2), 109–112. <https://doi.org/10.1038/ngeo2053>
- Rach, O., Kahmen, A., Brauer, A., & Sachse, D. (2017). A dual-biomarker approach for quantification of changes in relative humidity from sedimentary lipid D₁₈H ratios. *Climate of the Past*, 13(7), 741–757. <https://doi.org/10.5194/cp-13-741-2017>

- Rasmussen, S. O., Abbott, P. M., Blunier, T., Bourne, A. J., Brook, E., Buchardt, S. L., et al. (2013). A first chronology for the North Greenland Eemian Ice Drilling (NEEM) ice core. *Climate of the Past*, 9(6), 2713–2730. <https://doi.org/10.5194/cp-9-2713-2013>
- Reimer, P. J., Bard, E., Bayliss, A., Beck, J. W., Blackwell, P. G., Ramsey, C. B., et al. (2013). Intcal13 and Marine13 Radiocarbon Age Calibration Curves 0–50,000 Years Cal Bp. *Radiocarbon*, 55(4), 1869–1887.
- Rohling, E. J., & Pälike, H. (2005). Centennial-scale climate cooling with a sudden cold event around 8,200 years ago. *Nature*, 434(7036), 975. <https://doi.org/10.1038/nature03421>
- Russell, J. M., Hopmans, E. C., Loomis, S. E., Liang, J., & Sinninghe Damsté, J. S. (2018). Distributions of 5- and 6-methyl branched glycerol dialkyl glycerol tetraethers (brGDGTs) in East African lake sediment: Effects of temperature, pH, and new lacustrine paleotemperature calibrations. *Organic Geochemistry*, 117, 56–69. <https://doi.org/10.1016/j.orggeochem.2017.12.003>
- Sachse, D., Billault, I., Bowen, G. J., Chikaraishi, Y., Dawson, T. E., Feakins, S. J., et al. (2012). Molecular paleohydrology: Interpreting the hydrogen-isotopic composition of lipid biomarkers from photosynthesizing organisms. *Annual Review of Earth and Planetary Sciences*, 40(1), 221–249. <https://doi.org/10.1146/annurev-earth-042711-105535>
- Sachse, D., Radke, J., & Gleixner, G. (2004). Hydrogen isotope ratios of recent lacustrine sedimentary n-alkanes record modern climate variability. *Geochimica et Cosmochimica Acta*, 68(23), 4877–4889. <https://doi.org/10.1016/j.gca.2004.06.004>
- Schouten, S., Hopmans, E. C., Scheffuß, E., & Sinninghe Damsté, J. S. (2002). Distributional variations in marine crenarchaeotal membrane lipids: A new tool for reconstructing ancient sea water temperatures? *Earth and Planetary Science Letters*, 204(1), 265–274.
- Schweinsberg, A. D., Briner, J. P., Miller, G. H., Bennike, O., & Thomas, E. K. (2017). Local glaciation in West Greenland linked to North Atlantic Ocean circulation during the Holocene. *Geology*, 45(3), 195–198. <https://doi.org/10.1130/G38114.1>
- Screen, J. A., & Simmonds, I. (2012). Declining summer snowfall in the Arctic: Causes, impacts and feedbacks. *Climate Dynamics*, 38(11–12), 2243–2256. <https://doi.org/10.1007/s00382-011-1105-2>
- Shanahan, T. M., Hughen, K. A., & Van Mooy, B. A. S. (2013). Temperature sensitivity of branched and isoprenoid GDGTs in Arctic lakes. *Organic Geochemistry*, 64, 119–128. <https://doi.org/10.1016/j.orggeochem.2013.09.010>
- Shuman, B., Huang, Y., Newby, P., & Wang, Y. (2006). Compound-specific isotopic analyses track changes in seasonal precipitation regimes in the Northeastern United States at ca 8200 cal yr BP. *Quaternary Science Reviews*, 25(21–22), 2992–3002. <https://doi.org/10.1016/j.quascirev.2006.02.021>
- Sime, L. C., Risi, C., Tindall, J. C., Sjolte, J., Wolff, E. W., Masson-Delmotte, V., & et al. (2013). Warm climate isotopic simulations: What do we learn about interglacial signals in Greenland ice cores? *Quaternary Science Reviews*, 67(Supplement C), 59–80. <https://doi.org/10.1016/j.quascirev.2013.01.009>
- Skific, N., & Francis, J. (2013). Drivers of projected change in arctic moist static energy transport. *Journal of Geophysical Research: Atmospheres*, 118, 2748–2761. <https://doi.org/10.1002/jgrd.50292>
- Sodemann, H., Schwierz, C., & Wernli, H. (2008). Interannual variability of Greenland winter precipitation sources: Lagrangian moisture diagnostic and North Atlantic Oscillation influence. *Journal of Geophysical Research*, 113, D03107. <https://doi.org/10.1029/2007JD008503>
- Steen-Larsen, H. C., Masson-Delmotte, V., Sjolte, J., Johnsen, S. J., Vinther, B. M., Bréon, F.-M., et al. (2011). Understanding the climatic signal in the water stable isotope records from the NEEM shallow firn/ice cores in northwest Greenland. *Journal of Geophysical Research*, 116, D06108. <https://doi.org/10.1029/2010JD014311>
- Stuiver, M., Grootes, P. M., & Braziunas, T. F. (1995). The GISP2 $\delta^{18}\text{O}$ climate record of the past 16,500 years and the role of the Sun, ocean, and volcanoes. *Quaternary Research*, 44(3), 341–354. <https://doi.org/10.1006/qres.1995.1079>
- Sun, Q., Chu, G., Liu, M., Xie, M., Li, S., Ling, Y., et al. (2011). Distributions and temperature dependence of branched glycerol dialkyl glycerol tetraethers in recent lacustrine sediments from China and Nepal. *Journal of Geophysical Research*, 116, G01008. <https://doi.org/10.1029/2010JG001365>
- Teller, J. T., & Leverington, D. W. (2004). Glacial Lake Agassiz: A 5000 yr history of change and its relationship to the $\delta^{18}\text{O}$ record of Greenland. *GSA Bulletin*, 116(5–6), 729–742. <https://doi.org/10.1130/B25316.1>
- Thomas, E. K., Briner, J. P., Ryan-Henry, J. J., & Huang, Y. (2016). A major increase in winter snowfall during the middle Holocene on western Greenland caused by reduced sea ice in Baffin Bay and the Labrador Sea. *Geophysical Research Letters*, 43, 5302–5308. <https://doi.org/10.1002/2016GL068513>
- Thomas, E. K., Castañeda, I. S., McKay, N. P., Briner, J. P., Salacup, J. M., Nguyen, K., & et al. (2018). Data from Arctic hydroclimate intensification coincident with hemispheric warming 8,000 years ago [Database]. Retrieved July 6, 2018, from <https://www.ncdc.noaa.gov/paleo/study/24570>
- Thomas, E. K., Clemens, S. C., Prell, W. L., Herbert, T. D., Huang, Y., Liu, Z., et al. (2014). Temperature and leaf wax $\delta^2\text{H}$ records demonstrate seasonal and regional controls on Asian monsoon proxies. *Geology*, 42(12), 1075–1078. <https://doi.org/10.1130/G36289.1>
- Tierney, J. E., Schouten, S., Pitcher, A., Hopmans, E. C., & Sinninghe Damsté, J. S. (2012). Core and intact polar glycerol dialkyl glycerol tetraethers (GDGTs) in Sand Pond, Warwick, Rhode Island (USA): Insights into the origin of lacustrine GDGTs. *Geochimica et Cosmochimica Acta*, 77, 561–581. <https://doi.org/10.1016/j.gca.2011.10.018>
- Törnqvist, T. E., & Hijma, M. P. (2012). Links between early Holocene ice-sheet decay, sea-level rise and abrupt climate change. *Nature Geoscience*, 5(9), 601–606. <https://doi.org/10.1038/ngeo1536>
- Vaughan, D. G., Comiso, J. C., Allison, I., Carrasco, J., Kaser, G., Kwok, R., et al. (2013). Observations: Cryosphere. In T. F. Stocker, D. Qin, G.-K. Plattner, M. Tignor, S. K. Allen, J. Boschung, et al. (Eds.), *Climate change 2013: The physical science basis. Contribution of Working Group I to the Fifth Assessment Report of the Intergovernmental Panel on Climate Change*, (pp. 317–382). Cambridge, UK and New York, NY, USA: Cambridge Univ. Press.
- Vinther, B. M., Clausen, H. B., Fisher, D. A., Koerner, R. M., Johnsen, S. J., Andersen, K. K., et al. (2008). Synchronizing ice cores from the Renland and Agassiz ice caps to the Greenland Ice Core Chronology. *Journal of Geophysical Research*, 113, D08115. <https://doi.org/10.1029/2007JD009143>
- Weijers, J. W. H., Schouten, S., van den Donker, J. C., Hopmans, E. C., & Sinninghe Damsté, J. S. (2007). Environmental controls on bacterial tetraether membrane lipid distribution in soils. *Geochimica et Cosmochimica Acta*, 71(3), 703–713. <https://doi.org/10.1016/j.gca.2006.10.003>
- Werner, M., Heimann, M., & Hoffmann, G. (2001). Isotopic composition and origin of polar precipitation in present and glacial climate simulations. *Tellus B*, 53(1), 53–71. <https://doi.org/10.1034/j.1600-0889.2001.01154.x>
- Wrona, F. J., Johansson, M., Culp, J. M., Jenkins, A., Mård, J., Myers-Smith, I. H., et al. (2016). Transitions in Arctic ecosystems: Ecological implications of a changing hydrological regime. *Journal of Geophysical Research: Biogeosciences*, 121, 650–674. <https://doi.org/10.1002/2015JG003133>
- Young, N. E., & Briner, J. P. (2015). Holocene evolution of the western Greenland Ice Sheet: Assessing geophysical ice-sheet models with geological reconstructions of ice-margin change. *Quaternary Science Reviews*, 114, 1–17. <https://doi.org/10.1016/j.quascirev.2015.01.018>

- Young, N. E., Briner, J. P., Axford, Y., Csathó, B., Babonis, G. S., Rood, D. H., & et al. (2011). Response of a marine-terminating Greenland outlet glacier to abrupt cooling 8200 and 9300 years ago. *Geophysical Research Letters*, 38, L24701. <https://doi.org/10.1029/2011GL049639>
- Young, N. E., Briner, J. P., Rood, D. H., & Finkel, R. C. (2012). Glacier Extent During the Younger Dryas and 8.2-ka Event on Baffin Island, Arctic Canada. *Science*, 337(6100), 1330–1333. <https://doi.org/10.1126/science.1222759>
- Zhang, X., He, J., Zhang, J., Polyakov, I., Gerdes, R., Inoue, J., & et al. (2013). Enhanced poleward moisture transport and amplified northern high-latitude wetting trend. *Nature Climate Change*, 3(1), 47–51. <https://doi.org/10.1038/nclimate1631>